Stochastic multiresonance due to interplay between noise and fractals

S. Matyjaśkiewicz,[1,2,3] A. Krawiecki,[1] J. A. Hołyst,[1] and L. Schimansky-Geier[2]
[1]*Faculty of Physics and Center of Excellence for Complex Systems Research, Warsaw University of Technology, Koszykowa 75, 00-662 Warsaw, Poland*
[2]*Institute of Physics, Humboldt University at Berlin, Invalidenstrasse 110, D-10115 Berlin, Germany*
[3]*Department of Applied Mathematics, Warsaw Agricultural University, Nowoursynowska 166, PL-02-787 Warsaw, Poland*
(Received 14 March 2003; published 21 July 2003)

Stochastic multiresonance is shown to occur in a general class of threshold-crossing systems, in which a derivative of the threshold-crossing probability with respect to a system parameter is a nonmonotonic function of the noise intensity. As an example, a two-dimensional chaotic map is considered, where the threshold-crossing probability follows the overlap of the fractal structures of chaotic saddles and the basins of escape in noise-induced crisis. The analytic theory is in reasonable agreement with the numerical results for spectral power amplification.

DOI: 10.1103/PhysRevE.68.016216 PACS number(s): 05.45.−a, 05.40.−a

I. INTRODUCTION

Stochastic resonance (SR) is a phenomenon occurring in nonlinear systems whose response to a weak periodic stimulation is enhanced by addition of noise with optimum intensity [1–4]. This response can be characterized, e.g., by the spectral power amplification (SPA) defined as the ratio of the output signal power at the periodic stimulation frequency to the power of the input periodic signal. In systems with SR, the SPA shows maximum as a function of noise intensity. The occurrence of SR requires an energetic activation barrier or, more generally, a sort of threshold. The way in which this threshold is realized in the system dynamics and the suitable definition of the output signal, both enable distinction between the basic classes of systems exhibiting SR, such as bistable potential systems [5], dynamical [6] and nondynamical [7] threshold-crossing (TC) systems. A separate class of systems with SR is formed by chaotic systems without external noise, in which the internal chaotic dynamics can be tuned, by varying the control parameter, so that the output signal shows maximum periodicity [2,3,8]; this kind of SR is referred to as noise-free SR.

It has been recently realized that the picture of SR can be more complex than expected. In particular, in certain systems the output SPA can show multiple maxima as a function of the noise intensity, and the respective phenomenon was given a name stochastic multiresonance (SMR) [9–11] or was reported without referring to this name [12–19]. A similar phenomenon, noise-free SMR, was found in chaotic systems [20,21]. The ubiquity of SMR has been also confirmed by the recent experimental observations [22–25]. However, the theoretical investigations of SMR with noise have been so far constrained only to potential systems with certain discrete spatial symmetries [9,10] or with bistable potential and correlated noise [11].

In this paper, we propose a general class of TC systems in which multiple maxima of the SPA vs noise intensity appear in a natural way. We consider TC systems in which the TC probability depends on the noise intensity D and on some parameter q to which a weak periodic signal is added. We show that if the derivative of the TC probability with respect to q, considered as a function of the noise intensity, is nonmonotonic, the SMR appears in such TC systems, in the adiabatic limit of slow periodic signals. As a particular example of such a TC system we consider a two-dimensional chaotic map with noise-induced crisis [26], and with a periodic signal added to the control parameter q. In this example, SMR appears due to the fractal structures of attractors and the basins of attraction overlapping above the crisis point. For this case, we formulate an analytic theory for SMR based on the models of fractal attractors and their basins of attraction, valid for slowly varying periodic signals and correlated noise, which agrees qualitatively with the numerical results. The example analyzed extends the previous studies of noise-free SMR in maps with crises [20,21] to the case of noise-induced crises, i.e., to the case of SR with noise.

The rest of this paper is organized as follows. In Sec. II, we formulate a general theory which links the SPA with the derivative of the TC probability in the above-mentioned class of TC systems. In Sec. III, we introduce the model chaotic map, describe methods of analysis of SMR, and present an analytic theory for the SPA in two-dimensional chaotic maps close to the noise-induced crises (with details in the Appendixes). In Sec. IV, we present numerical evidence for the SPA with multiple maxima vs the noise intensity in the model map, and compare numerical and theoretical results. Finally, Sec. V contains conclusions.

II. STOCHASTIC MULTIRESONANCE IN THRESHOLD-CROSSING SYSTEMS: GENERAL CONSIDERATIONS

Let us consider a general class of TC systems in which the TC probability p depends on some parameter q and input noise with the intensity D, $p=p(q,D)$. A small periodic signal is added to the parameter q so that it becomes time dependent, $q(t)=q_0+q_1\cos(\omega t)$. Let us go to discrete time by dividing it into short time steps so that every TC event takes place within one time step. The output signal $y(t)$ is defined as $y(t)=1$ when at time t the TC event took place, and $y(t)=0$ otherwise. The output SPA σ is defined as

$$\sigma=\frac{|P_1|^2}{q_1^2}, \quad P_1=\lim_{N\to\infty}\frac{1}{NT}\sum_{t=1}^{NT} y(t)e^{i\omega t}, \tag{1}$$

where $T=2\pi/\omega$. If the TC system is nondynamical (i.e., we deal with static threshold nonlinearity), or if the TC system has internal dynamics but the periodic signal modulates it adiabatically, the TC probability becomes a periodic function of time which can be obtained as $p(t)=p(q_0+q_1\sin\omega t,D)$ and

$$P_1=\frac{1}{T}\sum_{t=1}^{T} p(t)e^{i\omega t}. \tag{2}$$

Assuming $q_1\ll 1$ and developing $p(t)$ in the Taylor series with respect to q yields in the first approximation

$$\sigma\approx|(\partial p/\partial q)|_{(q_0,D)}|^2/4. \tag{3}$$

From Eq. (3), it follows that a sufficient condition for the occurrence of SMR is that the derivative $\partial p/\partial q$, with fixed q_0, is nonmonotonic as a function of the noise intensity. The multiple maxima of the SPA are associated with extrema of this derivative. If the curve $p=p(q,D)$ is not differentiable with respect to q, one can replace the derivative in Eq. (3) with the difference quotient

$$p'(q_0,D)=[p(q_0+q_1,D)-p(q_0-q_1,D)]/2q_1. \tag{4}$$

III. THE MODEL AND METHODS OF ANALYSIS

A. Systems with crises as models for stochastic multiresonance

In order to introduce the model two-dimensional map close to noise-induced attractor merging crisis, let us start with the attractor merging crisis without noise. The attractor merging crisis [27,28] occurs in systems in which, for a range of values of the control parameter q, two symmetric chaotic attractors (henceforth called precritical attractors) exist with complementary precritical basins of attraction. As the control parameter is increased above the critical value q_c each attractor collides with a border of its precritical basin of attraction and pokes over it, overlapping the complementary basin. The precritical attractors are then turned into chaotic saddles, and their complementary basins of attraction into basins of escape. The phase trajectory bounces sequentially around the two saddles, occasionally jumping between them. The jump probability is proportional to the invariant measure of the chaotic saddle overlapping the basin of escape, and shows a trend given by a power scaling law $p(q)\propto(q-q_c)^{\tilde{\gamma}}$, where $\tilde{\gamma}>1/2$ is a critical exponent [27]. However, since the chaotic saddles inherit the fractal structure of the precritical attractors, with ragged distribution of the invariant measure, and the basins of escape can also have a fractal structure, significant oscillations of $p(q)$ superimposed on this trend can be often observed [28–30].

If the control parameter is below the critical value, $q<q_c$, merging of the precritical attractors is possible if noise with intensity D is added to the system; this phenomenon is called noise-induced attractor merging crisis. The fractal structures of the chaotic saddles and the basins of escape, although smeared out by noise, are still visible in the phase space. Thus, the jump probability $p(q,D)$ can still show oscillations around a certain main trend if q or D are varied [26]. Then the difference quotient $p'(q,D)$ can be a nonmonotonic function of the noise intensity D [note that since the oscillations of the jump probability are fractal induced, $p(q,D)$ need not be differentiable]. Hence, defining the TC events as jumps of the phase trajectory between the symmetric chaotic saddles, and adding periodic signal to the control parameter, we obtain a TC system fulfilling the sufficient condition given in Sec. II for the appearance of SMR.

B. The model of kicked spin map with noise

The TC system we take as an example is based on the chaotic kicked spin map. The map describes the motion of a classical magnetic moment (spin) $\mathbf{S}$, $|\mathbf{S}|=S$, in the field of uniaxial anisotropy and impulse transversal magnetic field $\tilde{B}(t)=B\Sigma_{n=1}^{\infty}\delta(t-n\tau)$ for which the Hamiltonian is $H=-A(S_z)^2-\tilde{B}(t)S_x$, where $A>0$ is the anisotropy constant. The time evolution of the spin is determined by the Landau-Lifschitz equation with damping constant λ. The equation can be integrated, and denoting the spin vector by $\mathbf{S}_n$ just after the nth field pulse one finds a two-dimensional map $\mathbf{S}_{n+1}=T[\mathbf{S}_n]$, whose form is given in Refs. [31–33].

For some regions of the model parameters, the spin map exhibits attractor merging crisis at $B=B_c$: for $B<B_c$ two separate symmetric chaotic attractors, corresponding to the spin "up" ($S_z>0$) and "down" ($S_z<0$) states, coexist, whereas for $B>B_c$ the attractors merge and the spin jumps between these two states. Both the chaotic saddles and the basins of escape are fractal, which is reflected in the TC probability $p(B)$, i.e., the probability of jump between the two spin orientations, which exhibits complicated oscillations around the power-law trend [29,30].

Keeping $B<B_c$, the noise-induced attractor merging crisis can be forced by adding noise to the system. In order to study SR in the spin map, a weak periodic signal and the noise $D\xi(n)$ is added to the control parameter B,

$$B(n)=B_0+D\xi(n)+B_1\cos(\omega n), \tag{5}$$

with the assumption that the noise has zero mean and $B_0+B_1<B_c$ to remain in the noise-induced crisis regime. Thus, $B_0-B_c\equiv q$ and $B_1\equiv q_1$ in the notation of Sec. II; since $\langle\xi(n)\rangle=0$, the parameters $B_0=\langle B(n)\rangle$ and D can be varied independently, as needed.

C. Methods of analysis

We simulate numerically the spin map with $B(n)$ given by Eq. (5), with various B_0, B_1, and D. The noise $\xi(n)$ has uniform distribution $\rho(x)=1/2$ on the interval $\langle-1,1\rangle$. Both white and correlated noise are considered. The correlated noise is obtained as follows. First, $\xi(0)$ is chosen at random. For $n\geqslant 1$, with probability Π the value of $\xi(n)$ is chosen at random, and with probability $1-\Pi$ it remains unchanged, $\xi(n)=\xi(n-1)$. The correlation time τ of this noise is of

order $1/\Pi$. The use of such correlated noise with uniform distribution makes possible the analytic studies in Sec. III D.

The model is treated as the TC system. The output signal is $y(n)=1$ if at time n the spin jump occurred, i.e., $S_{z,n}$ and $S_{z,n-1}$ have opposite signs, and $y(n)=0$ otherwise. From the output signal SPA is evaluated according to Eq. (1). Besides, for each B_0 the jump probabilities $p(B_0+B_1,D)$ and $p(B_0-B_1,D)$ are obtained numerically as functions of D, and the SPA is evaluated from Eqs. (4) and (3). A good agreement between both kinds of curves $\sigma(D)$ proves that our model is an example of the TC system supporting SMR, as described in Sec. II. Finally, the results are also compared with the analytic theory (see below, Sec. III D).

It should be mentioned that in the same map close to the attractor merging crisis, noise-free SMR was observed in Refs. [20,21]. In this paper, the study is extended to the case of crisis induced by noise, and SPA is not a function of the distance from crisis B_c-B_0 but the intensity of noise D. It should be also noted that SR with noise has already been studied in the spin map, but the amplitude of the periodic signal and noise intensities were too large to observe SMR due to the fractal structure of the precritical sets [34]. Besides, a related study of SR in the spin dynamics with continuous time [35] also did not show evidence for SMR.

D. Analytic theory for stochastic multiresonance in systems close to noise-induced crises

In this section, we present an analytic theory for SMR valid for two-dimensional maps close to noise-induced crises, with slow periodic signal and correlated noise. In contrast with the general considerations of Sec. II, the analytic theory for this particular case is based on the models of fractal chaotic saddle and basin of escape in the system close to crisis without noise, introduced in Refs. [29,30]. If the noise is strongly correlated and the periodic signal is slow, we assume that their effect is simply to vary in time the relative position of the chaotic saddles and the basins of escape, thus changing their overlap and the TC probability. In particular, we assume that the topological structure of these sets is not affected by the periodic signal and noise, and is identical with that of the corresponding precritical attractor and the basin of attraction.

We model the chaotic saddle with a set of parabolic branches $\mathcal{A}_k$, $k=1,2,\ldots K+1$, with a certain distribution of invariant measure $\tilde{\mu}_k$, and the basin of escape with a set of stripes $\mathcal{B}_l$, $l=1,2,\ldots,L+1$, where K and L define the accuracy of the finite approximation of the true fractal sets (Fig. 1). The distance between the top of the uppermost parabolic segment $\mathcal{A}_{K+1}$ and the lower boundary of the lowermost stripe $\mathcal{B}_{L+1}$ is given by the control parameter q. If the correlated noise and the slow periodic signal are added to the control parameter so that $q(n)=q_0+q_1\cos(\omega n)+D\xi(n)$, then the measure of the overlap between the chaotic saddle and the basin of escape becomes slowly time dependent. Then the instantaneous value of the jump probability is proportional to a sum of contributions from the overlap between the parabolic segments $\mathcal{A}_k$ and the stripes $\mathcal{B}_l$,

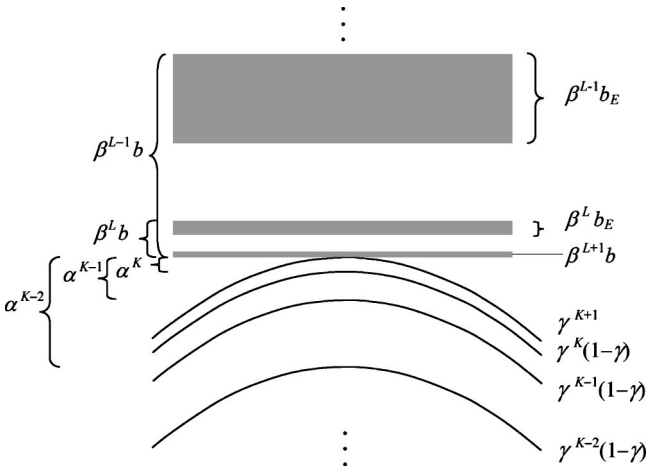

FIG. 1. The model of the fractal chaotic saddle and the basin of escape. The tops of the parabolic segments of the saddle $\mathcal{A}_k$ are located at $y=(1-\delta_{k,K+1})a\alpha^k+q$ and their relative invariant measures are given by $\tilde{\mu}_k=(1-\gamma)\gamma^k$, for $0\leqslant k\leqslant K$, and $\tilde{\mu}_{K+1}=\gamma^{K+1}$. The lower and upper boundaries of the stripes of the basin are located at $y=(1-\delta_{l,L+1})(\beta^l b-\beta^l b_E)$ and $y=\beta^l b$, respectively. The figure shows the location of parabolic segments and stripes for $q=0$.

$$p^{(inst)}(n)=\zeta\sum_{k=0}^{K+1}\sum_{l=0}^{L+1}\mu_{kl}^{(inst)}(n), \tag{6}$$

where $\mu_{kl}^{(inst)}(n)$ is the instantaneous measure of $\mathcal{A}_k$ inside $\mathcal{B}_l$ at time n and ζ is the proportionality constant.

After simple calculations (see Appendix A), using Eqs. (A1), (A2), and (A3), the periodic in time jump probability $p(n)$ can be easily obtained by averaging $p^{(inst)}(n)$ over the noise distribution. This averaging procedure resembles the one used in Ref. [26] to obtain universal scaling behavior for the jump probability in noise-induced crises. On the basis of Eq. (6), the Fourier coefficient (2) can be then written as

$$P_1=\zeta\sum_{k=0}^{K+1}\sum_{l=0}^{L+1}M_{kl,1}, \tag{7}$$

where $M_{kl,1}$ are the Fourier coefficients at frequency ω of the measures $\mu_{kl}^{(inst)}(n)$ averaged over the noise distribution, i.e., of the quantities $\mu_{kl}(n)$ from Eq. (A3). The analytic form of $M_{kl,1}$ is given in Appendix B. The theoretical curve SPA vs D can be plotted after inserting P_1 into Eq. (1). The form of the above result resembles that of SPA in noise-free SMR in two-dimensional maps close to the crisis [20]. The SPA is independent of ω, which is typical of the TC systems in the adiabatic limit.

IV. RESULTS AND DISCUSSION

A. Evidence for stochastic multiresonance due to collision of fractal sets

In this section, we present numerical results for SPA vs D obtained in the system discussed in Sec. III B, and compare

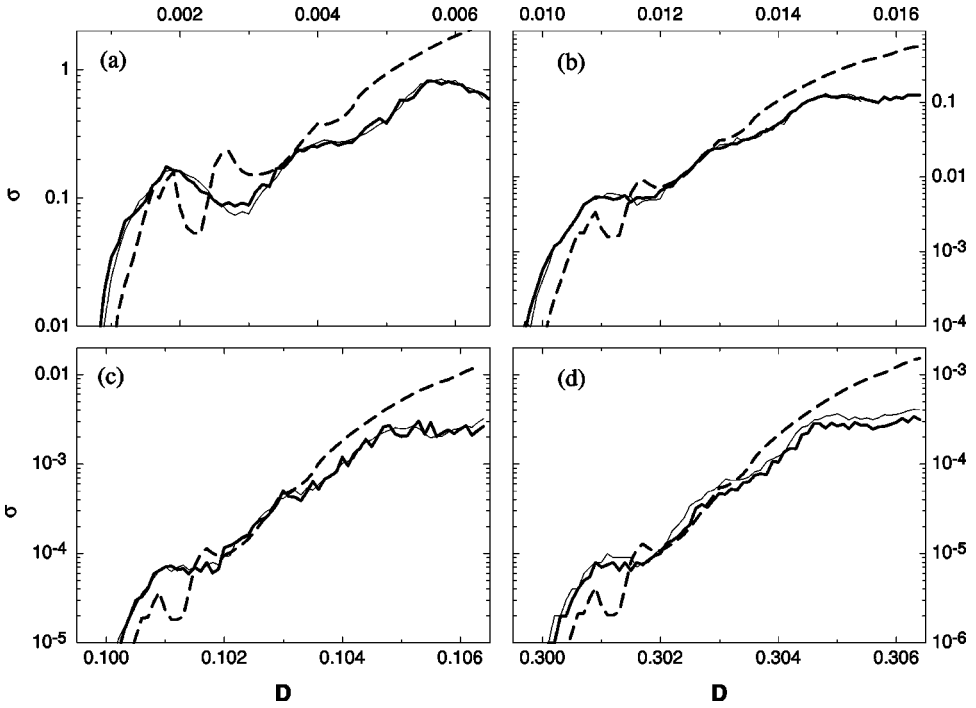

FIG. 2. SMR in the spin map for the crisis parameters $S=1$, $A_c=1$, $\tau_c=2\pi$, $\lambda_c=0.105\,494\,12\ldots$. Numerical results: σ vs D for $B_1=6\times10^{-4}$, $\tau=10$, and (a) $B_0=0.999$, (b) $B_0=0.99$, (c) $B_0=0.9$, (d) $B_0=0.7$ (thick solid line); SPA evaluated from numerical escape probability—thin solid line; SPA obtained from fractal model developed in Sec. III D with parameters $\alpha=0.0108$, $\gamma=0.294$, $\beta=0.125$, $b_E=1.467\,93$, $a=4.5009$, $b=2.7$, $\zeta=3.33$, and $K=L=10$ is shown by the dashed line.

them with the theoretical results. In Fig. 2, typical σ vs D curves are shown, obtained from numerical simulations with various distances B_c-B_0 from the crisis point. In Fig. 2(a), SPA exhibits two strong maxima and a plateau located between them, thus SMR is found. With increasing B_c-B_0, the maxima of the SPA become smoother and the maxima at smaller D are turned into plateaus [Figs. 2(b)–2(d)], but the shape of the SPA curves is always different from a typical one with a single maximum. In all cases, nonzero SPA was observed for $B_0+B_1+D>B_c$; taking into account that $B_0+B_1<B_c$, we observe SMR in the parameter regime of the noise-induced attractor merging crisis.

The direct stemming of the complicated structure of the SPA curves from the nonmonotonic derivative $p'(B_0,D)$ is well visible in Fig. 2. Here, the numerical SPA obtained from the output signal is compared with the SPA obtained from the numerical TC probability as described in Sec. III C, using Eqs. (4) and (3). Figure 2 shows very good agreement between the two kinds of curves, i.e., σ vs D for all B_0-B_c. This result confirms directly that the map under study belongs to the class of TC systems supporting SMR, introduced in Sec. II. The SPA as a function of B_0 and D, evaluated from the numerical TC probability, is shown also in Fig. 3 as a three-dimensional plot, for easier comparison of σ vs D curves for various B_0.

In Fig. 2, the numerical results are also compared with the analytic ones, based on the theory of Sec. III D, with the parameters obtained similarly as in Refs. [20,21]. The theoretical σ vs D curves for all distances B_c-B_0 agree qualitatively with the numerical ones. The best agreement is obtained for small D and B_c-B_0. This is because the models of the fractal sets in Fig. 1 are approximate; they capture well the structure of the chaotic saddle and basin of escape just above the crisis point, but do not take into account all details of the fractal sets and their possible changes with increasing noise. This qualitative agreement confirms indirectly that the SMR is in fact connected with the overlap between the fractal chaotic saddles and the basins of escape above the noise-induced crisis point.

B. Changes of the spectral power amplification with increasing distance from the crisis point

Let us discuss briefly the differences between σ vs D curves for increasing distance B_c-B_0. The basic effect is the decrease of σ as the distance B_c-B_0 increases. Besides, the height of the maxima of the SPA at smaller D diminishes faster than that of the maxima at larger D (Figs. 3 and 2). These effects are very intuitive, and result from the overall decrease of the spin jump probability with increasing B_c-B_0. For decreasing B_0, larger noise intensity D is required to induce the crisis, the density of the noise $D\xi$, $\rho(D\xi)=1/2D$ becomes lower, and the probability that ξ is in the range where noise can induce spin jumps, i.e., that B_c-B_0

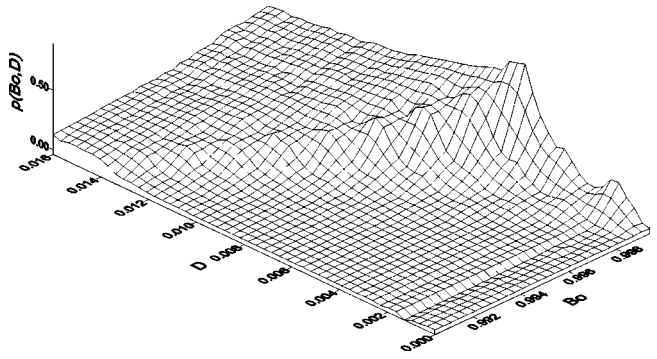

FIG. 3. SMR in the spin map with parameters from Fig. 2. SPA evaluated the from numerical escape probability as a function of noise intensity D and control parameter B_0 for $B_1=6\times10^{-4}$ and $\tau=10$.

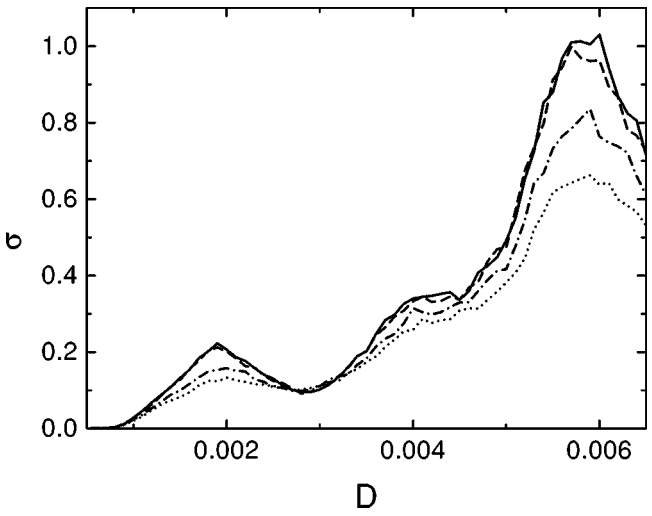

FIG. 4. Influence of the noise correlation time on SMR in the spin map with parameters from Fig. 2 and noise correlation times: $\tau=100$ (solid line), $\tau=10$ (dashed line), $\tau=5$ (dash-dotted line), $\tau=2$ (dotted line).

$-B_1<D\xi<D$, is smaller. The decrease of the spin jump probability results in the overall decrease of the SPA according to Eqs. (2) and (1). Moreover, let us assume that the maximum value of the control parameter (5), $B_0+B_1+D>B_c$, is fixed. Then, the closer this quantity is to B_c, the larger are the relative changes of the spin jump probability with decreasing B_0. As a consequence, SPA decreases in general faster at smaller D than at larger D when the distance from the crisis point is increased, which explains the relative diminishing of the maxima of the SPA at smaller noise intensities. Both tendencies are also well captured by the theory given in Sec. III D.

Another effect, already mentioned in the proceding seciton, is smoothing of the maxima of the SPA and turning them into plateaus with the rise of B_c-B_0. This effect is not predicted by the theory given in Sec. III D, which suggests that it is related to smearing out the fractal structures of the chaotic saddles and the basins of escape by increasing noise, that is needed to induce crisis with rising B_c-B_0. This smearing can be a dynamical phenomenon, not taken into account by the adiabatic theory. It can be, e.g., related to the transient effects, since for large D the phase trajectory needs long time to relax after each large change of $\xi(n)$. The above results show that the fractal structures of chaotic saddles and the basins of escape are reflected in the complex shape of the σ vs D curves in noise-induced crises, leading to SMR. However, increasing noise smears out the effect of these structures by smoothing the maxima of the SPA and decreasing their height as B_c-B_0 increases. In the limit of large D and B_0-B_c, one should expect smooth σ vs D curves with a single maximum, as in Ref. [34]. Nevertheless, for small periodic signals, even in this case remnant effects of the underlying fractal structures can still be observed, as in Fig. 2(d).

The general shape of the SPA in Figs. 2 and 3 resembles the phenomenon ''tuning without noise'' [36–38]. It happens in large ensembles of stochastic resonators with independent noise, but driven by a small subthreshold signal common to all elements. The signal-to-noise ratio and the other measures of SR in such devices exhibit a broad maximum if plotted with respect to the noise strength. As the number of elements tends to infinity, the subthreshold signal passes the ensemble perfectly, which is a consequence of the law of large numbers. In such ensembles a large number of attractors exists with a widely distributed spectrum of possible escape rates between the several attractors. It makes the ensemble able to respond efficiently to the subthreshold periodic driving in a broad window of noise intensities.

Similarly, in our system, for moderate noise the signal is amplified due to the existence of multiple possible transition paths between the two spin orientations, starting from the distinct segments of the chaotic saddles. For fixed B_0 and B_1, the system is able to find a possible transition path between the two chaotic saddles, corresponding to the overlap of a certain segment of the saddle (widened by noise) with the basin of escape. For higher noise, a large number of branches of the saddle overlaps the basin of escape, thus the signal is amplified due to a large number of possible transitions in a broad window of noise intensities. Hence, SPA vs D curve exhibits a plateau as a result of transitions between different branches of the symmetric chaotic saddles.

C. Changes of the spectral power amplification with the noise correlation time

In Fig. 4, we analyze the SPA as a function of noise intensity for various noise correlation times $\tau\equiv 1/\Pi$ (Fig. 4). For $\tau=100$ and $\tau=10$, the SPA has almost the same value; small differences result from numerical errors. This confirms that the correlation time we used for simulations in Fig. 2 was long enough to fulfill the criteria for applicability of the theory given in Sec. III D. For shorter correlation times $\tau=5$ and $\tau=1$ (white noise), the SPA becomes smaller, but maxima are still well visible. Hence, the SMR due to the overlap of fractal sets appears even for uncorrelated noise, in the limit where the analytic theory in Sec. III D is already not valid.

D. Changes of the spectral power amplification with the amplitude of the periodic signal

In Fig. 5, the SPA as a function of noise intensity for increasing amplitudes of the periodic signal is shown. For $B_1=3\times10^{-4}$ and $B_1=6\times10^{-4}$ [Figs. 5(a) and 5(b)], the multiple maxima of σ are well visible, and the analytical results based on the topological model predict well the location of the first maximum. With the signal amplitude increasing up to $B_1=12\times10^{-4}$, the multiple maxima merge; analogous phenomenon was observed in the case of noise-free SMR [20]. This shows that SMR due to the interplay between noise and fractals is strongly dependent on the amplitude of periodic signal. For large amplitudes, only one maximum of the SPA is observed, and the SMR turns into ''conventional'' SR [34].

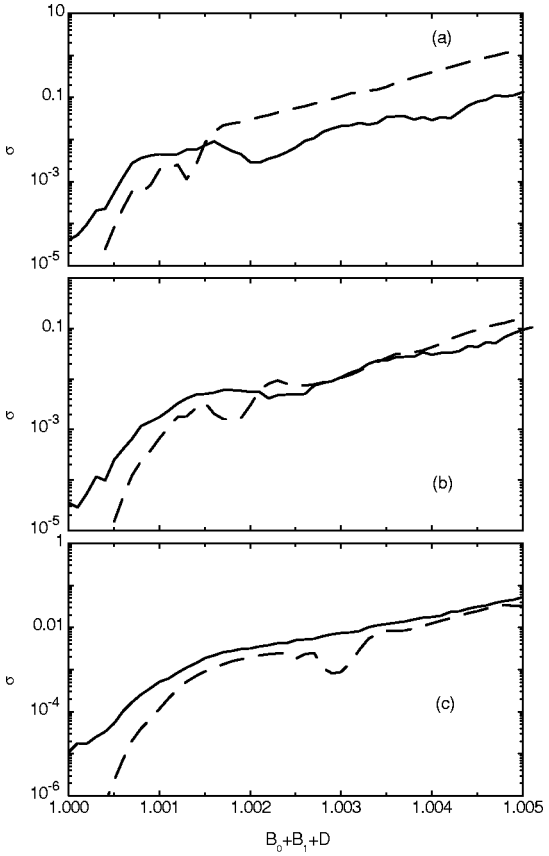

FIG. 5. Influence of the amplitude of the periodic signal on SMR in the spin map with parameters from Fig. 2, $B_0=0.99$ and amplitudes $B_1=3\times10^{-4}$ (a), $B_1=6\times10^{-4}$ (b), $B_1=12\times10^{-4}$ (c). Numerical results—solid line, analytic results—dashed line.

V. CONCLUSIONS

In this paper, we study the phenomenon of SMR which appears in a natural way in a general class of TC systems. It is shown that the multiresonance occurs due to the nonmonotonic derivative of the TC probability with respect to some parameter q, which the periodic signal is added to, considered as a function of the noise intensity. We have studied the spin map, where this derivative is nonmonotonic due to the fractal structures of the chaotic saddles and basins of escape colliding above the noise-induced crisis point. For such a case, we propose an adiabatic theory combined with a topological model for colliding fractal sets, which yields the SPA curves in qualitative agreement with the numerical results. The latter results are an extension of our previous investigation of noise-free SMR in this system. We also pointed out some analogy between our model and the phenomenon ''tuning without noise.'' Since oscillations of the TC probability were observed in many systems with crises [39], the results for the spin map suggest that SMR can be observed also in other numerical and experimental chaotic systems close to crises. However, our theory is not constrained only to this class of systems; the relationship between the nonmonotonic derivative of the TC probability and the appearance of SMR is a universal condition leading to SMR in TC systems.

ACKNOWLEDGMENTS

This work was supported by the Polish Committee for Scientific Research under Grant No. 5 P03B 007 21. S.M. acknowledges financial support from the DAAD Programme during his stay at the Institute of Physics, Humboldt University at Berlin.

APPENDIX A: THE MEASURE OF THE FRACTAL CHAOTIC SADDLE IN THE BASIN OF ESCAPE

The instantaneous measure $\mu_{kl}^{(inst)}(n)$ in Eq. (6) is

$$\mu_{kl}^{(inst)}(n)=\mu_{k}^{(inst)}[(1-\delta_{l,L+1})(\beta^l b-\beta^l b_E),n]-\mu_{k}^{(inst)}[\beta^l b,n], \tag{A1}$$

where $\mu_{k}^{(inst)}(c,n)$ is the instantaneous measure of $\mathcal{A}_k$ inside a half plane $y>c$. For small distance between the top of the parabolic segment and the half-plane border, $q(n)-(1-\delta_{k,K+1})a\alpha^k-c\ll1$, the measure $\mu_{k}^{(inst)}[c,n]$ can be approximated by the square root:

$$\mu_{k}^{(inst)}(c,n)=\tilde{\mu}_k[q_0+q_1\cos(\omega n)+D\xi(n)-(1-\delta_{k,K+1})a\alpha^k-c]^{1/2}\Theta(q_0+q_1\cos(\omega n)+D\xi(n)-(1-\delta_{k,K+1})a\alpha^k-c), \tag{A2}$$

where Θ denotes the Heaviside function.

In order to obtain the periodic in time jump probability $p(n)$ introduced in Sec. II, we assume that the correlation time of the noise is significant, but still small in comparison with the period of the periodic signal. For the noise defined in Sec. III C, this means $1\ll1/\Pi\ll T$, which is in reasonable agreement with the conditions for the numerical simulations in Figs. 2, 3, and 5. Due to the separation of time scales, the instantaneous measure $\mu_{k}^{(inst)}[c,n]$ can be first averaged over the uniform noise density $\rho(\xi)=1/2$ to yield the periodic in time averaged measure of the parabolic segment $\mathcal{A}_k$ inside the half plane $y>c$,

$$\mu_k(c,n)=\int_{-1}^{1}d\xi\rho(\xi)\mu_{k}^{(inst)}(c,n)=\frac{\tilde{\mu}_k}{3D}[q_0+q_1\cos(\omega n)+D-(1-\delta_{k,K+1})\times a\alpha^k-c]^{3/2}\Theta(q_0+q_1\cos(\omega n)+D-(1-\delta_{k,K+1})a\alpha^k-c). \tag{A3}$$

In this way, $p(n)$ is obtained on the average of $p^{(inst)}(n)$ from Eq. (6) over the noise distribution.

APPENDIX B: EVALUATION OF THE SPECTRAL POWER AMPLIFICATION

Our goal is to evaluate the Fourier coefficient (2) from $p(n)$. To perform calculations analytically, let us go from discrete to continuous time. Since we are interested in the

noise-induced crisis, there is $q_0+q_1<0$, and we take $c \geqslant 0$. Let us introduce the quantities

$$Q=q_0-(1-\delta_{k,K+1})a\alpha^k,$$

$$m=\left(\frac{2q_1}{Q+q_1+D-c}\right)^{1/2},$$

$$\hat{t}=\begin{cases} \omega^{-1}\arccos\left(\dfrac{c-D-Q}{q_1}\right) & \text{if } \dfrac{c-D-Q}{q_1}>-1 \\ T/2 & \text{if } \dfrac{c-D-Q}{q_1}<-1, \end{cases} \tag{B1}$$

where for $0<t<\hat{t}$ and $T-\hat{t}<t<T$, there is a nonzero probability of overlap between the top of the parabolic segment $\mathcal{A}_k$ and the half plane $y>c$ after adding noise and periodic signal to the control parameter q. Then the Fourier coefficient at frequency ω of the periodic in time measure $\mu_k(c,n)$ (A3) is

$$M_{k,1}(c)=\frac{1}{T}\int_0^T \mu_k(c,t)\cos(\omega t)dt$$

$$=\frac{2\tilde{\mu}_k}{3\pi D}(Q+q_1+D-c)^{3/2}\left[\frac{2(m^4-m^2+1)}{5m^2}\right.$$

$$\left.\times E\left(\frac{\omega\hat{t}}{2},m\right)+\frac{-m^4+3m^2-2}{5m^2}F\left(\frac{\omega\hat{t}}{2},m\right)\right]$$

$$\times\Theta(Q+q_1+D-c), \tag{B2}$$

where $F(\phi,m)$ and $E(\phi,m)$ are elliptic integrals of the first and the second kind, respectively. Then, using Eq. (A1), we get the Fourier coefficient of the measure of the parabolic segment $\mathcal{A}_k$ inside the strips $\mathcal{B}_l$, averaged over the noise intensity as

$$M_{kl,1}=M_{k,1}[(1-\delta_{l,L+1})(\beta^l b-\beta^l b_E)]-M_{k,1}(\beta^l b), \tag{B3}$$

which should be substituted in Eq. (7) to obtain P_1 analytically.

[1] R. Benzi, A. Sutera, and A. Vulpiani, J. Phys. A **14**, L453 (1981).
[2] L. Gammaitoni, P. Hänggi, P. Jung, and P. Marchesoni, Rev. Mod. Phys. **70**, 223 (1998).
[3] V.S. Anishchenko, S. Neiman, F. Moss, and L. Schimansky-Geier, Physics-Uspekhi (Russia) **42**, 7 (1999) [Usp. Fiz. Nauk **169**, 7 (1999)].
[4] F. Moss, in *Self-Organized Biological Dynamics & Nonlinear Control*, edited by J. Walleczek (Cambridge University Press, Cambridge, 2000), p. 236.
[5] B. McNamara and K. Wiesenfeld, Phys. Rev. A **39**, 4854 (1989).
[6] K. Wiesenfeld, D. Pierson, E. Pantazelou, Ch. Dames, and F. Moss, Phys. Rev. Lett. **72**, 2125 (1994).
[7] Z. Gingl, L.B. Kiss, and F. Moss, Europhys. Lett. **29**, 191 (1995).
[8] V.S. Anishchenko, A.B. Neiman, and M.A. Safanova, J. Stat. Phys. **70**, 183 (1993).
[9] J.M.G. Vilar and J.M. Rubí, Phys. Rev. Lett. **78**, 2882 (1997).
[10] J.M.G. Vilar and J.M. Rubí, Physica A **264**, 1 (1999).
[11] J. Wang, L. Cao, and D.J. Wu, Eur. Phys. J. B **29**, 123 (2002).
[12] P. Jung and P. Hänggi, Phys. Rev. A **44**, 8032 (1991).
[13] Kwan-tai Leung and Z. Néda, Phys. Lett. A **246**, 505 (1998).
[14] Kwan-tai Leung and Z. Néda, Phys. Rev. E **59**, 2730 (1999).
[15] B.J. Kim, P. Minnhagen, H.J. Kim, M.Y. Choi, and G.S. Jeon, Europhys. Lett. **56**, 333 (2001).
[16] F. Chapeau-Blondeau, Phys. Rev. E **61**, 940 (2000).
[17] L. Gammaitoni, Phys. Rev. E **52**, 4691 (1995).
[18] R.A. Wannamaker, S.P. Lipschitz, and J. Vanderkooy, Phys. Rev. E **61**, 233 (2000).
[19] D.T.W. Chik, Yuquing Wang, and Z.D. Wang, Phys. Rev. E **64**, 021913 (2001).
[20] S. Matyjaśkiewicz, A. Krawiecki, J.A. Hołyst, K. Kacperski, and W. Ebeling, Phys. Rev. E **63**, 026215 (2001).
[21] A. Krawiecki, S. Matyjaśkiewicz, K. Kacperski, and J.A. Hołyst, Phys. Rev. E **64**, 041104 (2001).
[22] Z. Hou, L. Yang, and H. Xin, J. Chem. Phys. **111**, 1592 (1999).
[23] M.I. Tsindlekht, I. Felner, M. Gitterman, and B.Ya. Shapiro, Phys. Rev. B **62**, 4073 (2000).
[24] Y.H. Shiau and Z. Néda, Jpn. J. Appl. Phys., Part 1 **40**, 6675 (2001).
[25] Zhang ji-Qian and Xin Hou-Wen, Chinese Phys. Lett. **18**, 870 (2001).
[26] J.C. Sommerer, E. Ott, and C. Grebogi, Phys. Rev. A **43**, 1754 (1991).
[27] C. Grebogi, E. Ott, and J.A. Yorke, Phys. Rev. Lett. **57**, 1284 (1986).
[28] C. Grebogi, E. Ott, F. Romeiras, and J.A. Yorke, Phys. Rev. A **36**, 5365 (1987).
[29] K. Kacperski and J.A. Hołyst, Phys. Lett. A **254**, 53 (1999).
[30] K. Kacperski and J.A. Hołyst, Phys. Rev. E **60**, 403 (1999).
[31] J.A. Hołyst and A. Sukiennicki, Acta Phys. Pol. A **81**, 353 (1992).
[32] J.A. Hołyst and A. Sukiennicki, J. Magn. Magn. Mater. **104-107**, 2111 (1992).
[33] K. Kacperski and J.A. Hołyst, Phys. Rev. E **55**, 5044 (1997).
[34] S. Matyjaśkiewicz, J.A. Hołyst, and A. Krawiecki, Phys. Rev. E **61**, 5134 (2000).
[35] A. Pérez-Madrid and J.M. Rubí, Phys. Rev. E **51**, 4159 (1995).
[36] F. Moss and X. Pei, Nature (London) **376**, 211 (1995).
[37] D. Chialvo, A. Longtin, and J. Müller-Gerking, Phys. Rev. E **55**, 1798 (1997).
[38] A. Neiman, L. Schimansky-Geier and F. Moss, Phys. Rev. E **56**, R9 (1997).
[39] J.C. Sommerer and C. Grebogi, Int. J. Bifurcation Chaos Appl. Sci. Eng. **2**, 383 (1992).